Journal of Materials Chemistry A

Accepted Manuscript

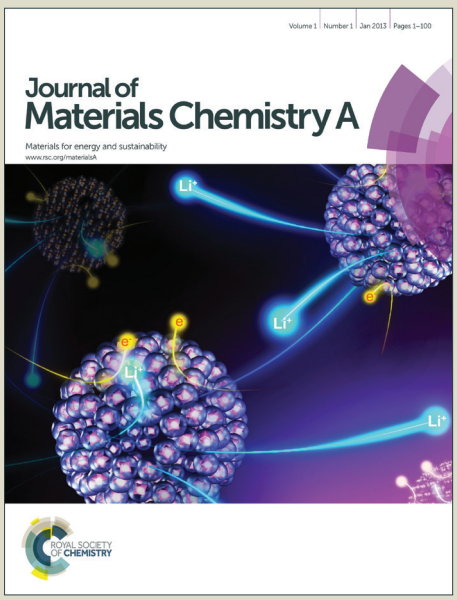

ROYAL SOCIETY OF CHEMISTRY

www.rsc.org/materialsA

Journal of Materials Chemistry A RSCPublishing

ARTICLE

Assessing the potential of metal oxide semiconducting gas sensors for illicit drug detection markers†

Cite this: DOI: 10.1039/x0xx00000x

P. Tarttelin Hernández[a], A. J. T. Naik[b], E. J. Newton[a], and S. Hailes[c], I. P.Parkin[*b]

Received 00th January 2014,
Accepted 00th January 2014

DOI: 10.1039/x0xx00000x

www.rsc.org/

Port security with a focus on drug trafficking prevention requires inexpensive and portable systems for on-site analysis of containers in order to minimise transit delays. The potential of metal oxide semiconductors for illicit drug detection is explored here. A six-sensor array consisting of WO_3 and SnO_2 inks was devised. Zeolites H-Y and H-ZSM-5 were incorporated to introduce variations in sensor response. Sensors were tested against acetone, ethanol and toluene as proxies for their use in illicit drug manufacture and against ammonia and nitrogen dioxide as first models of amino- and nitro-containing compounds, given their prevalence in the structural framework of drugs and precursor molecules. Sensor sensitivity and selectivity were greatly enhanced by inclusion of zeolite materials. Admixed sensing materials were found to be particularly sensitive to the gases. Support Vector Machines were applied to the dataset as classification tools that accurately classified the data according to gas type. The sensing array was successful in targeting and discerning between the tested drug markers. This could be key for illicit drug detection with electronic noses based on MOS technology in the future.

Introduction

Drug trafficking poses one of the biggest threats to society with severe health, economic and political implications worldwide.[1-3] Maritime drug trafficking poses a particularly pressing challenge for the authorities due to high volume of goods being transported by sea.[4, 5] A number of reports have recently highlighted the need to develop improved technologies for illicit drug detection in freight.[1, 5, 6] In order to improve current technologies, port security needs inexpensive and portable systems that facilitate the on-site analysis of containers in multiple locations to minimise transit delays.

Metal oxide semiconducting (MOS) gas sensors have been the subject of growing research interest for the detection of low-volatility contraband materials like explosives but their application in illicit drug detection has been largely disregarded.[7-9] Despite the high sensitivity, low cost and portability benefits associated with MOS sensors, they are restricted in their selective capabilities[10-13] and the particularly low vapour pressure of most drugs makes their precise and selective detection challenging.[14-16] The incorporation of zeolites as catalytic and filtering materials is being extensively investigated as a means to improve specificity and sensitivity of sensors.[17-21] The fundamental drawback of selectivity can be overcome by using an integrated array of different sensors, each of them providing a different response to any given target gas.[22-24] The combined response of the array, called an e-nose, may then provide the necessary specificity and sensitivity for the gas detection being sought. The collection of individual signals provided by each sensor of the array can then be compiled and translated into a unique fingerprint of the gas, with the help of classifying techniques like Support Vector Machines (SVM).[7, 25]

The aim of this study was to explore MOS gas sensors as a means of detecting solvents used in drug manufacture and functional groups prevalent in the structural framework of drugs as proxies of the drugs themselves. This was achieved by exploring the use of WO_3 and SnO_2 sensors, modified by admixture or overlay of H-ZSM-5 and H-Y zeolites. The sensitivity of these was tested against acetone, ammonia, ethanol, toluene and nitrogen dioxide for the following reasons. Acetone, ethanol and toluene are common solvents employed in drug manufacture.[26-28] Ammonia may be thought as a first model of amine groups that abound in drugs of abuse, and ammonia is also sought as an indicator of methamphetamine production in clandestine labs.[26, 27] Nitrogen dioxide is a model for nitro groups that are found in some precursor molecules and in novel and dangerous drugs of abuse.[4, 26] Previous research has shown that sensors that are sensitive to nitrogen dioxide are also sensitive to nitro-containing

compounds[7] and it is anticipated that in future research the same can be achieved for other nitro- and amino- containing compounds. Physicochemical characterisations (XRD, SEM, EDX, Raman) were performed prior and after gas exposure to examine differences in sensing materials and the effect of gas and heat exposure. SVM was used as a classifier of the different sensor responses for the purpose of gas recognition.

By introducing zeolites into the sensing material, sensor responses are far greater than that which has previously been achieved in other studies. This therefore enables the detection of illicit drugs to be tackled with MOS gas sensors.

2. Materials and Methods

2.1 Material Preparation

Gas sensing materials were made from commercial WO_3 (New Metals Chemicals Ltd.) and SnO_2 powders (Aldrich). Zeolite powders were obtained from Zeolyst International, USA (NH_4-ZSM-5 CBV 8014 and Y-zeolite CBV 600). Both zeolites were employed in the hydrogen form. H-ZSM-5 zeolite was prepared by firing at 100 °C for 8 hours to remove moisture and subsequently firing it at 500 °C for 12 hours to prompt de-ammoniation. Y-zeolite was already supplied in the hydrogen form and thus was not subjected to any treatment prior to use.

Metal Oxides with Zeolite Overlays and Admixtures

Metal oxides were mixed with an organic vehicle (ESL400, Agmet Ltd.) and ground with a pestle and mortar to produce homogeneous inks for screen-printing. Inks were screen-printed onto 3×3 mm alumina substrates that have inter-digitated gold electrodes on the obverse and heater tracks on the reverse. Screen-printing was carried out using a DEK 1202 screen printer. Unmodified sensors were made up of 4 layers of either WO_3 or SnO_2, without adjunction of zeolite. Film thickness is known to affect sensor sensitivity; although no published studies have been found that specifically investigate the effects of film thickness of MOS on the performance of the sensors, Varsani et al (2011) and Peveler et al (2013) reported 4 and 5 ink depositions of the control sensing material that provided excellent sensing results. The ink was allowed to dry under an infrared lamp for 10 minutes between depositions. Zeolite inks were prepared by mixing the powders with the organic vehicle. Overlays consisted of two additional film applications over the sensing materials. Zeolite admixtures were prepared by mixing the metal oxides and zeolite powders with the ESL400 vehicle. Six sensors were developed as shown in Table 1. The strip thereby obtained was cut down into individual sensor chips, which were then calcined in a quartz crucible in a Carbolite CSF 1200 furnace at 600 °C for 1 h to burn off the organic vehicle and strengthen the attachment of the ink to the gold electrodes.

Table 1 Sensor abbreviation and description. The number of layers printed is specified in parentheses. After the sensor name 'Y' refers to H-Y zeolite, 'ZSM' refers to H-ZSM-5 zeolite, 'over' refers to overlay and 'admix' refers to admixture.

Sensor Abbreviation	Sensing Material	Overlays
SnO_2	SnO_2 (4)	Nil
WO_3	WO_3 (4)	Nil
SnO_2 + Y admix	SnO_2, 30% Y (4)	Nil
WO_3 + Y over	WO_3 (4)	Y zeolite (2)
WO_3 + HZSM5 over	WO_3 (4)	H-ZSM-5 (2)
WO_3 + HZSM5 admix	WO_3, 30% HZSM5 (4)	Nil

Platinum wires were afterwards spot-welded onto gold spots on the sensor chip, and were then used to connect the sensor on brass pins in moulded polyphenylene sulphide housings. Spot welding was performed on a MacGregor DC601 parallel gap resistance welder.

2.2 Sensor Characterisation

Sensor characterisation was performed prior to and after gas testing to look for potential transformations in sensing materials. X-Ray diffraction (XRD) was carried out on a Bruker D8 discover diffractometer with a copper X-ray source operating at 30 W with a Vantec 500 detector. XRD patterns were collected over the 2θ range 15 - 45°, with a time step of 100 s/step and using a 0.3 mm collimator.

Energy dispersive X-ray spectroscopy (EDX) was carried out for elemental analysis with an Oxford Instruments INCA energy system in conjunction with a Phillips XL30 environmental scanning electron microscope (SEM).

Top-down SEM images were obtained using a JEOL 6301F scanning microscope with an accelerating voltage of 4.0 kV. Carbon coating of the samples prior to SEM was performed on an Edwards S105B sputter-coater. Secondary electron imaging of sensors was performed using a Hitachi S-3400 N SEM.

Raman Spectroscopy was executed on a Renishaw inVia microscope using a 325 nm excitation laser. Normalisation was performed in order to better compare peak shapes amongst spectra.

2.3 Gas testing rigs and protocol

Gas sensing experiments were performed on a gas-sensing rig in the UCL Department of Chemistry, using 6 sensors at a time.

Sensor resistance is recorded by means of a potential divider circuit and analogue-to-digital converter card.[7] The integrated heater tracks on the sensors were heated to 300 °C, 350 °C, 400 °C and 450 °C. Gas flow is controlled through mass flow controllers (MFC) that provide a total flow of 1000 cm^3/min. Solenoid valves are in place to control the

introduction of the test gas to the main stream of air. Dry air is purged through the system for a period of two hours prior to exposing the sensors to different gases to avoid cross-contamination and to settle the baseline. In this period, the sensors are heated to 500 °C to desorb any residual gas from the sensor surface.

A typical experiment consisted of an initial 20-minute pulse of dry air to determine the baseline response of the sensors (R_0). Five 10-minute pulses of test gas were then introduced at increasingly varied concentrations ranging between 5-60% of the original cylinder concentration, namely ethanol (100 ppm), acetone (10 ppm), toluene (50 ppm), ammonia (50 ppm) and nitrogen dioxide (1 ppm). The sensors were allowed to return to baseline in-between gas pulses with a 14-minute pulse of dry air. Test gases were obtained from BOC Gases.

Sensor sensitivity was calculated by comparing the resistance of the sensor when exposed to the test gas (R) to that in air (R_0). In the case of an increase in resistance (resistive response) the response is calculated as R/R_0, whereas a decrease in resistance (conductive response) it is calculated as R_0/R. The magnitude of response is calculated as S = Rmax – R_0. Where 'Rmax' is the maximum sensitivity of the sensor. The complete sensor array included unmodified SnO_2, SnO_2 admixed with H-Y, unmodified WO_3, WO_3 admixed with H-ZSM-5, WO_3 overlaid with H-ZSM-5 and WO_3 overlaid with H-Y.

2.4 Support Vector Machine

Support vector machines or SVMs are learning models able to analyse multidimensional data and recognise patterns. SVMs assume that the dataset belong to either of two classes, the elements of which can be separated by a hyperplane in data space such that all elements particular to one class will fall under the same side of the plane. The SVM is a maximum margin classifier, determining the equation of the optimal hyperplane by maximising the distance between the closest points in the dataset.[29-31]

In more realistic scenarios, the classes may not be linearly separable. SVM then transforms the original input space into a higher dimensional feature space, after which the optimal linear separating hyperplane is sought.[29] In this report, a Sequential Minimal Optimisation (SMO) SVM provided by the WEKA software (University of Waikato, New Zealand) has been used as a classifier for gas recognition.

3. Results & Discussion

3.1 Sensor Characterisation

Sensors were fabricated by screen-printing WO_3 and SnO_2 material inks onto alumina substrates and were modified by admixture or overlay of zeolites H-ZSM-5 and H-Y as depicted in Fig. 1. Following ink deposition the sensors were fired at 600 °C for one hour to evaporate the organic vehicle used to produce the printable ink and to sinter the material onto the substrate. Physicochemical characterisation globally showed that the structure of the materials remained unaltered after exposing the sensors to heat and to test gases.

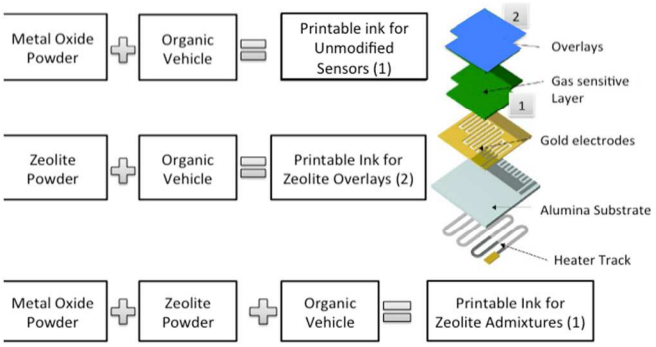

Fig. 1. Schematic of sensor fabrication process used in this study. Unmodified sensors were made by subsequently printing four layers of the same sensing material (1). Overlays were made by screen-printing additional depositions of zeolite on the surface of the unmodified sensing material (2). Admixtures were made my mixing the zeolite powder with the metal oxide powder together with the vehicle and printing 4 layers of the material on the alumina substrate as per (1). Image adapted from G. F. Fine et al.[32]

3.1.1 X-Ray Diffraction

This analysis confirmed that the structure of the metal oxides and zeolites remained unaltered after calcination or exposing the sensors to test gases (Fig. 2). XRD patterns revealed that WO_3 was present in a monoclinic form with characteristic 2θ peaks at 23.16°, 23.65°, 24.4°, 33.2°. SnO_2 was tetragonal in structure with characteristic 2θ peaks at 26.5°, 33.8° and 51.7°. H-Y-zeolite displayed a cubic structure with

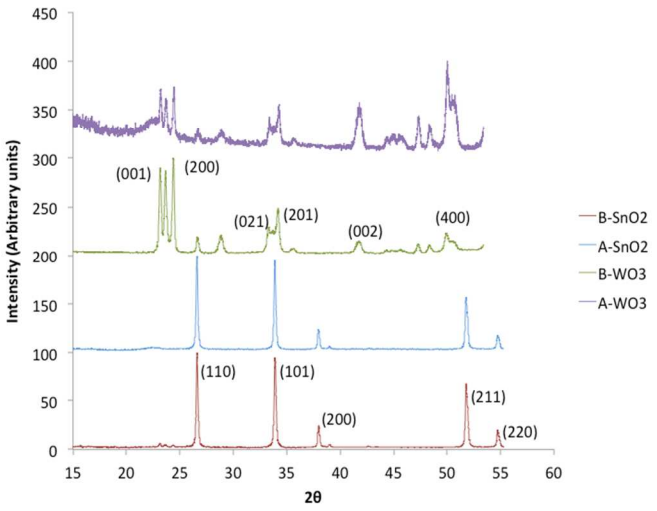

Fig. 2. XRD patterns of tungsten oxide and tin oxide sensors collected before 'B' and after 'A' gas exposure collected between 2θ range 15 and 45°. Principal peaks have been indexed according to standards attained from the literature.

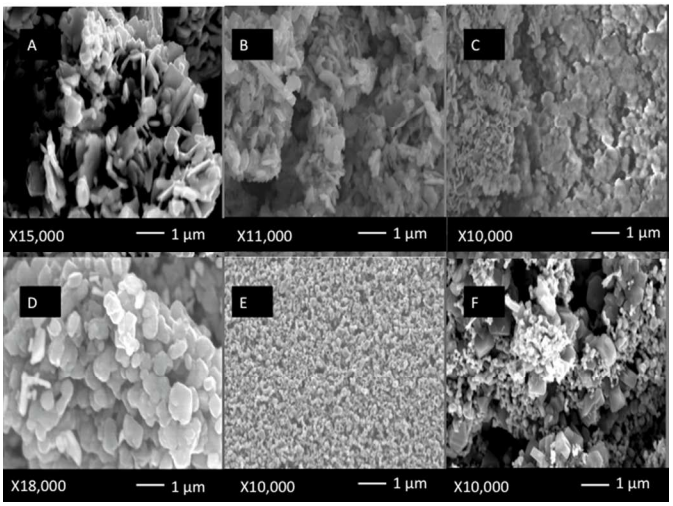

Fig. 3. SEM images of tungsten and tin oxide sensors before gas exposure. 'A' WO_3, 'B' WO_3 + H-ZSM-5 admix, 'C' WO_3 + H-ZSM-5 overlay, 'D' WO_3 + Y zeolite overlay. 'E' SnO_2, 'F' SnO_2 + Y zeolite admix'.

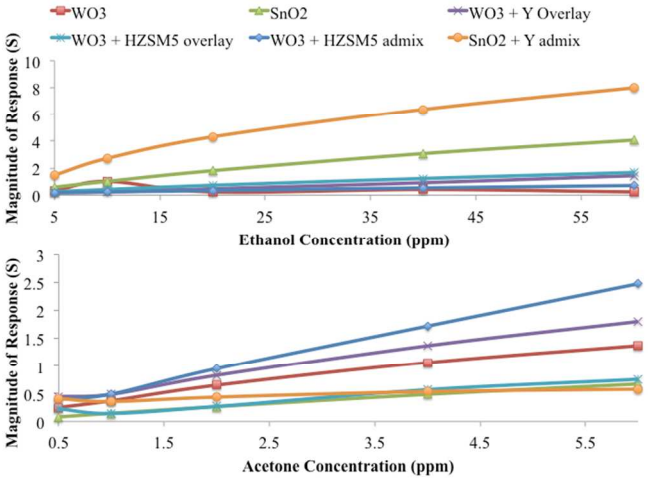

Fig. 4. Magnitude of sensor responses (S = R_{max} - R_0) to ethanol (top) when exposed to concentrations ranging between 5 and 60 ppm at 300 °C, and to acetone gas (bottom) when exposed to concentrations ranging between 0.5 and 6 ppm at 350 °C. These temperatures were selected as they provided the highest sensitivity to ethanol and acetone, respectively.

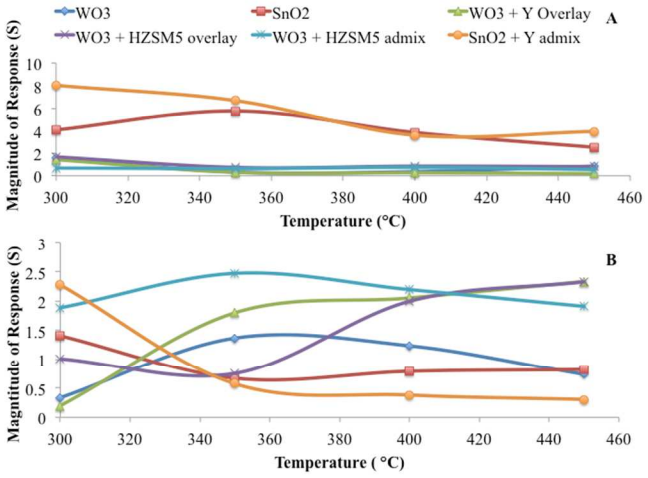

Fig. 5. Magnitude of sensor responses (S = R_{max} – R0) to (A) 60 ppm Ethanol and (B) 6 ppm acetone gases when heated to 300 °C, 350 °C, 400 °C and 450 °C.

peaks at 2θ 10.27°, 12.04°, 15.87° and 22.23° and H-ZSM-5 showed a MFI structure with peaks at 2θ 7.9°, 8.8°, 14.7° and 23.05°. Note that while the sensors overlaid with zeolite showed more intense peaks for the zeolite, admixtures only showed trace amounts of zeolites.

3.1.2 Scanning Electron Microscope

SEM images were taken at ×27, ×10,000, x11,000, ×15,000, x18,000, ×20,000 and ×40,000 magnifications. Fig. 3 presents a collection of images corresponding to tungsten and tin oxide sensors prior to gas exposure. No change was observed in the surface structures before and after exposing the sensors to gases.

Control WO_3 sensors present a flake-like appearance with grains generally being 1µm in size. H-ZSM-5 zeolite admixtures and overlays show a more fluffy appearance, with a less apparent flake-type structure. The structure of the overlaid sensors looks uniformly flat (Fig. 2C), as opposed to the more lumpy and porous appearance of the unmodified sensors and admixtures. The structure of the Y-zeolite overlaid sensor presents clusters of grains that are spherical in shape and much smaller in size than those of H-ZSM-5, with some grains being less than 100 nm.

SnO_2 sensors present a distinct round shape of approximately 100 nm in size. The typical structure of H-ZSM-5 zeolite can be recognised and more clearly discerned in the overlay images than in the admixtures. This is also the case for the images corresponding to H-Y zeolite.

3.1.3 Raman Spectroscopy

Tungsten sensors show bands at 720 cm^{-1} and 810 cm^{-1}. These bands are characteristic of WO_3. Note that after gas exposure sensors 'A-WO_3 + Y overlay' and 'A-WO_3 + H-ZSM5 overlay' presented an extra band at 940 cm^{-1}. This may suggest a change in the crystalline structure of the materials.

The intensities of the tungsten oxide sensors were higher than those of tin oxide sensors. Tin oxide sensors showed two peaks at approximately 460 cm^{-1} and 610 cm^{-1}. These bands are characteristic of SnO_2. †

3.1.4 Energy Dispersive X-Ray Spectroscopy

Energy dispersive X-ray analysis (EDX) was used to carry out elemental analysis of the sensors. Zeolite-overlaid WO_3 sensors have low tungsten content at their surface while admixtures show a much-increased presence of this element, as

expected. No differences in the elemental analysis of the sensors were found before and after exposure to gases. †

3.2 Results on Reducing Gases

The sensors were exposed to five different concentrations of each gas ranging between 5 and 60% of their cylinder concentrations. Ethanol, acetone, toluene and ammonia are reducing gases and they interact with n-type semiconductors to show a decrease in resistance (conductive response R_0/R).

All sensors adhered to this behaviour except when exposed to ammonia; the sensors showed a p-type response with the exception of 'SnO_2 + Y admix' at temperatures 300 – 400 °C. The sensors showed a decrease in resistance consistent with n-type semiconductors at 450 °C. This behaviour is not uncommon in MOS sensors; it is thought to be caused by the accumulation of water vapour at the sensor surface.[33]

Sensor sensitivity generally increased with concentration of test gas (Fig. 4). Sensitivity was found to be highest at 300 °C when exposed to ethanol and 350 °C when exposed to acetone (Fig. 5). Nevertheless, SnO_2 sensors were more sensitive to acetone at 300 °C. Contrary to the trend observed for the other reducing gases tested, the sensitivity of sensors to toluene and ammonia was greatest at 400 °C and 450 °C, respectively.

Table 2 illustrates the effect of zeolite incorporation on the sensor response, that is, whether fast or slow reactions take place at the sensor surface and sensor sensitivity. Essentially, a shark-fin transient shape indicates a slow response of the sensor and failure to reach steady state at the supplied test gas concentrations. A slower response is often seen in the modified sensors; the incorporation of zeolite results in a longer diffusion time through the pores of the zeolite. Conversely, a flattened sensor response shape is indicative of a fast reaction occurring at the surface of the sensing material. A flattened response could also be indicative of poor sensitivity to the reaction products.

Zeolite incorporation was found to introduce variability in the sensor responses. When an enhancement is seen in the sensor responses of the zeolite-modified sensor over that of the unmodified sensor it can be an indication that reaction products are formed to which the sensing material is more sensitive; the high porosity and surface area of zeolites generates more surface reactive sites that enable the gases to rapidly diffuse through the pores in the zeolite, resulting in an improvement in the conductivity of the sensing material.[34] The converse is true when a diminution is observed in the sensor response of the zeolite-modified sensor. As an example, a 2-fold enhancement in sensor response was observed in the SnO_2 modified sensor when compared to the unmodified one when the sensors are exposed to 60 ppm ethanol. When exposing the sensors to 6 ppm of acetone gas, the 'WO_3 + HZSM5 admix' sensor provided the highest magnitude of response ($S = 2.4$), a 1.8-fold increase over the response of the unmodified sensor. The super-cage found in H-Y zeolite (window 7.4 Å, cage 13.2 Å) favours the absorption of acetone onto its cavity,[35] which justifies the increase in response observed in the WO_3 + Y overlaid zeolite. In the case of sensor exposure to 30 ppm toluene, 'WO_3 + HZSM5 admix' and 'SnO_2 + Y admix' showed a 3.2-fold and a 7-fold increase in response, respectively, over the unmodified sensors. Note that 'WO_3 + HZSM5 admix' and 'WO_3 + HZSM5 overlay' sensors often showed different behaviours. This could be the result of the gas diffusing more readily through the pores of the zeolite in the case of the overlay.

It is suggested that the reaction pathways in schemes 1- 4 may occur at the surface of the MOS material when exposed to ethanol, acetone, toluene and ammonia, respectively:[13, 36-39]

Ethanol

$C_2H_5OH\ (gas) + O^- \rightarrow CO_2 + H_2O + e^-$ (Sch. 1.0)

$CO_2\ (gas) + e^- \rightarrow CO^{2-}$ (Sch. 1.1)

$CO^{2-} + O^- + 2e^- \rightarrow CO\ (gas) + 2O^{2-}$ (Sch. 1.2)

Acetone

$CH_3COCH_3\ (gas) + OH- \rightarrow CH_3CHO + CH_3$ (Sch. 2.0)

$CH_3COCH_3\ (gas) + O^- \rightarrow [CH_3COCH_2]^+ + OH^- + e^-$ (Sch. 2.2)

$CH_3CHO + O\ (bulk) \rightarrow CH_3COOH + O\ (vacancies)$ (Sch. 2.3)

Or

$CH_3COCH_3 + O^- \rightarrow [CHCO] + CHO^- + e^-$ (Sch. 2.4)

$CH_3CO \rightarrow [CH_3]+ + CO$ (Sch. 2.5)

$CO + O- \rightarrow CO_2 + e^-$ (Sch. 2.6)

Toluene

$C_6H_5CH_3\ (gas) + 18O^- \rightarrow 7CO_2\ (gas) + 4H_2O\ (gas) + 18e^-$ (Sch. 2.7)

Ammonia

$2NH_3\ (gas) + 3O^-\ (ads) \rightarrow N_2 + 3H_2O + 3e^-$ (Sch. 3.0)

$2NH_3\ (gas) + 5O^-\ (ads) \rightarrow 2NO + 5e^-$ (Sch. 3.1)

$2NH_3\ (gas) + 4O^-\ (ads) \rightarrow N_2O + 3H_2O + 4e^-$ (Sch. 3.2)

Table 2 – Sensor sensitivity (S) to the highest supplied concentration of ethanol, acetone, toluene and ammonia gas at their most sensitive temperatures. The shape of the transient pulse has been described using '+' to emphasise the property that is being defined. 'Eth' refers to ethanol, 'acet' to acetone, 'tol' to toluene and 'amm' to ammonia.

	Test Gases							
	Eth (60 ppm, 300 °C)		Acet (6 ppm, 350 °C)		Tol (30 ppm, 450 °C)		Amm (30 ppm, 450 °C)	
Sensors	Transient	*S*	Transient	*S*	Transient	*S*	Transient	*S*
SnO_2	Shark fin +	4.08	Flat + baseline drift	0.67	Flat	0.33	Flat	0.25
WO_3	Flat +	1.55	Flat	1.37	Shark fin +	2.18	Shark fin +, baseline drift ++	1.50
SnO_2 + Y admix	Shark fin	8.02	Peak decline	0.58	Shark fin	8.79	Flat, baseline drift ++	1.01
WO_3 + Y over	Flat +	1.44	Flat	1.80	Flat	1.08	Shark fin	0.95
WO_3 + HZSM5 over	Flat +	1.68	Flat	0.76	Flat	0.39	Shark fin	0.28
WO_3 + HZSM5 admix	Flat +	0.72	Shark fin	2.48	Shark fin	9.33	Shark fin +, baseline drift ++	1.31

Sensor sensitivity can be primarily explained by a change in the concentration of adsorbed oxygen species at the surface of the sensing material upon exposure to a gas, which results in a change in conductivity. However, in the case of ethanol, these reaction pathways could also explain the higher responses attained with the SnO_2 sensors as previous studies have shown their sensitivity towards CO gas.[36] This reaction pathway would also explain the low responses attained for WO_3 sensors as they have been previously shown to be poorly sensitive to CO gas.[13]

The low sensor responses to acetone gas could be explained by the second reaction pathway (2.4); Wetchakun et. al (2011)[36] provide an account on MOS detection of hazardous gases such as CO_2. In the paper they highlight that although modified and unmodified SnO_2 sensors are sensitive to concentrations of CO_2 (1000 - 3000 ppm) at temperatures in the 100 – 350 °C range, the magnitude of response to CO_2 is very low (S = ~1.4 to 2500 ppm of gas).

Upon exposure to toluene gas, it was only the modified SnO_2 sensor that was found to be particularly sensitive to the reaction products of toluene. Given that WO_3 is known to be poorly sensitive to CO_2 and in this study high responses were attained for the unmodified WO_3 sensor (S = 4.9) when exposed to 60 ppm of toluene at 400 °C it is suggested that a different reaction pathway occurs at its surface.

Baseline drift and peak tailing were observed when the sensors were exposed to toluene and ammonia. Ammonia has been said to chemisorb at the sensor surface due to its high affinity with zeolite materials,[36] and it is possible that toluene also behaves in a similar fashion. Nevertheless, this could also be the result of water vapour accumulation on the surface of the sensor,[33] although this is unlikely at such high temperatures.

3.3 Results on Oxidising Gas

The sensors were exposed to NO_2 concentrations ranging between 50 and 600 ppb. NO_2 is an oxidising gas that results in an increase in the resistance of n-type semiconductors. Sensor sensitivity was found to progressively increase when exposed to higher concentrations of the gas. The sensors were sensitive to nitrogen dioxide at the ppb level, showing the highest sensitivity at 300 °C (Fig. 6). WO_3 sensor responses were significantly improved by the introduction of zeolites, particularly zeolite H-ZSM-5. Upon exposure to 600 ppb of NO_2, the 'WO_3 + HZSM5 overlay' sensor showed a 4.4-fold increase over that of unmodified WO_3, which is considerably lower than other reported studies.[7, 13]

Metal oxide conductivity is believed to be driven, primarily, by Schottky-type potential barriers occurring at the grain boundaries of the sensor film in the presence of oxygen molecules.[40] A modification in the concentration of adsorbed species at the surface of the sensor film, triggered in this instance by oxidising gas molecules, cause conduction band electrons to immobilise, hence creating more surface acceptor states that result in a change in the conductivity of the sensing material. In fact, NO_2 is thought to chemisorb onto the surface of the material, abstracting electrons, as opposed to reacting with the oxygen ions found at the surface, as follows:[13]

$$NO_2 + 1e^- \rightarrow NO_2^- \qquad \text{(Sch. 4.0)}$$

At 300 °C the transients had a shark-fin shape suggestive of a catalytic reaction occurring at the sensor surface. The unmodified WO_3 sensor responded faster than the zeolites modified by admixture or overlay. This is due to a percolation effect affecting the diffusion of the gas through the zeolite layers.

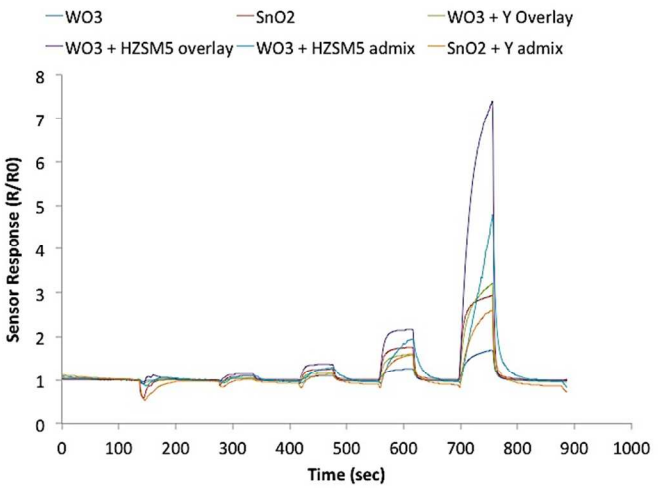

Fig. 6 Response transients to 50 ppb, 100 ppb, 200 ppb, 400 ppb and 600 ppb nitrogen dioxide at 300 °C.

The increase in sensor response observed with the incorporation of H-ZSM-5 zeolite is a result of the increased surface area of the pore microstructures. This zeolite has been reported to react with NO_2 molecules to give products to which the underlying WO_3 is more sensitive.[7, 13]

The unmodified SnO_2 sensor was more sensitive to NO_2 than the unmodified WO_3 sensor. This was unexpected due to the recognised affinity of WO_3 sensors to NO_2. The SnO_2 sensor modified by admixture with zeolite H-Y responded more slowly than the unmodified sensor and it was also less sensitive to NO_2. Nevertheless, the responses of the SnO_2 sensors were very similar in magnitude regardless of temperature and concentration.

3.4 Overview of Sensing Results

The sensitivity and discriminating power of the sensors modified with zeolites has been greatly improved in contrast to the sensitivity of the unmodified sensors; a 2-fold enhancement was observed in the sensor response of the modified SnO_2 sensor when compared to the unmodified one upon exposure to 60 ppm ethanol; exposure to 6 ppm acetone gas resulted in sensor 'WO_3 + HZSM5 admix' providing the highest magnitude of response (S = 2.4), a 1.8-fold increase over the response of the unmodified sensor and a 1.6-fold enhancement was observed in the SnO_2 modified sensor over that of the control. Sensors 'WO_3 + HZSM5 admix' and 'SnO_2 + Y admix' showed a 3.2-fold and a 7-fold increase in response, respectively, over the unmodified sensors when exposed to 30 ppm of toluene gas.

In the case of testing against ethanol, acetone and ammonia, the sensitivity was also improved over that of other studies reported in the literature, which used similar sensor fabrication methodologies.[7, 34, 41, 42] Studies on the detection of toluene with SnO_2 and WO_3 modified with zeolites have not been reported in the literature. Sensor responses to NO_2 with H-ZSM-5 adjunction were considerably lower than reported studies in the literature.[7, 13] The film thickness (four layers) used in this study was comparatively lower to that reported in other studies, which may have consequently affected sensor sensitivity.[7]

Doped SnO_2 sensors have previously been shown to be greatly sensitive to ethanol; Ma et al[41] recently reported sensor responses of doped SnO_2 of R_0/R = ~10 to 100 ppm ethanol at 300 °C. The sensor responses that have been attained here for unmodified and modified SnO_2 sensors corresponded to R_0/R = ~ 11 and ~ 9.3 at 60 ppm. There has been less focus on the properties of WO_3 for ethanol detection. Nevertheless, M. Ahsan et al[42] reported sensor responses of thin film WO_3 sensors of R_0/R = ~0.79 at 150 °C. The sensitivity of WO_3 sensors modified with H-ZSM-5 and H-Y zeolites provided responses of R_0/R = 2.8 and R_0/R = 2.5 at 300 °C, respectively.

Previous studies that looked to detect 5 ppm acetone at 350 °C with thick-film WO_3 sensors reported responses (R_0/R) of ~2.2 for zeolites H-ZSM-5 and LTA doped with chromium and they reported responses of 1.6 for WO_3 overlaid with H-ZSM-5 zeolite.[34] Here, the zeolite-modified sensors have provided responses of 3.6 when admixed with H-ZSM-5 and of 2.9 when overlaid with zeolite H-Y.

The literature on toluene detection with thick-film MOS sensors is limited. Toluene detection has, in the past, been explored with NiO/Fe_2O_3 thick films[43], and with NiO-SnO_2 composite nanofibres.[39] More recently toluene detection has been explored with NiO[44] and ZnO nanowires[45] and with WO_3 nanostructures. Studies based on ZnO nanowires attained responses that were very low in comparison to what was found here. Nevertheless, studies exploring NiO nanowires and Pd-doped WO_3 nanostructures, attained considerably higher responses R_0/R = 7.8 to 5 ppm and R_0/R = 6 to 1 ppm toluene,[44, 46] respectively, showing great promise for toluene detection.

Other studies looking to detect ammonia with thick-film MOS sensors have also reported difficulties in attaining a stable baseline and in getting the sensors to return to baseline.[7]

3.5 Results of the Support Vector Machines

An SVM training algorithm was used to build a model to classify a subgroup of the data collected according to class, that is, according to the gas being tested. An SMO approach was used to train the SVM.[7, 29, 30] Multi-class problems are solved using a one-versus-one strategy.

A model was built to see if the SVM could successfully classify acetone, toluene, ethanol and nitrogen dioxide based on the complete sensor array. The dataset was comprised of 7679 data points including maximum resistive and conductive responses at the supplied gas concentrations for all the temperatures tested. Sensor sensitivity (R_0/R and R/R_0) collected at five 10-second increments following gas injection was also included in the dataset.

The training model was built using an RBF kernel with default values C = 250007 and γ = 0.01. It was found that the SMO training model was more accurate in correctly classifying the gases when the WEKA cost function 'c' and cross-validation values were subsequently increased. The algorithm could correctly classify the data 89.79% of the time when using a 30-fold cross validation and c = 100000. To reduce the likelihood of overfitting, we tried a number of other classifiers based on a J48 decision tree and obtained similar performance. As can be seen in the confusion matrix shown in Table 3 below, the two gases that were most confounded were ethanol and toluene. Conversely, the gas that was less confounded was nitrogen dioxide. This can be attributed to its resistive response, thus facilitating its identification.

Table 3. Confusion matrix corresponding to an SMO algorithm using an RBF Kernel with parameters C = 250007 and γ = 0.01. A 30-fold cross validation was used to build the model. This model was 89.79% accurate in classifying the gases.

a	b	c	d	← Classified as
99	2	19	0	a = Ethanol
4	111	2	3	b = Acetone
14	5	101	0	c = Toluene
0	0	0	120	d = Nitrogen Dioxide

Although the sensing performances of MOS tested in this study have proven successful in discriminating amongst the gases tested, it would be worth investigating the incorporation of other sensing materials such as p-type semiconductors to introduce further variation in the sensing responses. This could consequently improve the classification accuracy of the models and would further support the suitability of MOS gas sensors as e-noses for the purposes of illicit drug detection. Nevertheless, it remains key to validate the methodologies currently used to fabricate and test MOS gas sensors so that they can indeed be used reliably for security applications.

4.0 Conclusions

This study has evaluated the viability of using a six gas-sensor array based on MOS for the detection of markers of illicit drugs and precursor molecules such as solvents and functional groups prevalent in their structural framework.

It has been illustrated here that MOS gas sensors are successful in targeting solvents relevant to illicit drug manufacture. In future research, this could be key to illicit drug detection with e-noses.

Generally, zeolite admixtures were found to be particularly good at improving the sensitive and selective capabilities of the sensing materials. Although the sensing responses to acetone were not particularly high, WO_3 based sensors were found to be more sensitive to acetone than SnO_2 sensors; both SnO_2 sensors were particularly sensitive and selective towards ethanol; 'SnO_2 + Y admix' and 'WO_3 + HZSM5 admix' sensors were shown to be greatly sensitive to toluene; the sensors were also very sensitive to nitrogen dioxide, with sensitive detection at the ppb level, and it is expected that they will be responsive to other nitro-containing compounds as reported in the literature. The sensor responses to ammonia persistently showed baseline instability at lower temperatures. Nevertheless, the incorporation of zeolite materials proved to enhance the magnitude of responses of the otherwise unmodified sensors. Further research is needed to assess whether the sensor array would be successful in detecting amine-containing compounds.

SVM was used as a classifier of a subset of the data and it effectively differentiated sensor responses according to gas type with model accuracy of > 89 %.

These results are very encouraging and support the need to further explore the use of MOS as e-noses for illicit drug detection.

Acknowledgements

The authors acknowledge Professor David Williams for his insight and advice and Steve Firth, Kevin Reeves and Martin Vickers for their technical support. Financial support was provided by the EPSRC grant code EP/G037264/1 as part of UCL's Security Science Doctoral Training Centre.

Notes

[a] Dept. of Security and Crime Science, University College London, 35 Tavistock Sq., London, WC1H 9EZ, UK

[b] Dept. of Chemistry, University College London, 20 Gordon St, London, WC1H 0 AJ, UK. Email: i.p.parkin@ucl.ac.uk, Fax: +44 (0)20 7679 7463; Tel: +44 (0)20 7679 4669

[c] Dept. of Computer Science, University College London, Gower St., London, WC1E 6BT, UK

Supplementary information (S1) of Raman spectra of WO_3 and SnO_2 sensors before and after gas exposure have been included. (S2) EDX of the sensors have also been included.

References

1. T. McSweeney, P. J. Turnbull, M. Hough, "Tackling Drug Markets and Distribution Networks in the UK. *A review on recent literature*" *ISBN: 978-1-906246-06-8* (2008).
2. O. Akiba, International trade in narcotic drugs. *Futures* **29**, (1997) 605.
3. M. Singer, Drugs and development: The global impact of drug use and trafficking on social and economic development. *International Journal of Drug Policy* **19**, (2008) 467.
4. United, Nations, "World Drug Report" (United Nations Office on Drugs and Crime, Vienna, Austria, 2013).

5. UnitedNationsOfficeonDrugsandCrime, "The UNODC-WCO container control programme" (2006).
6. HMGovernment, "Drug Strategy 2010; Reducing demand, restricting supply, building recovery: supporting people to live a drug free life" (London, 2010).
7. W. J. Peveler, R. Binions, S. M. V. Hailes, I. P. Parkin, Detection of explosive markers using zeolite modified gas sensors. *Journal of Materials Chemistry A* **1**, (2013) 2613.
8. D. S. Lee *et al.*, Explosve gas recognition system using thick film sensor array and neural network. *Sensors and Actuators B* **71**, (2000) 90.
9. A. A. Vasiliev, V. V. Malyshev, Sensors for the ultra-fast monitoring of explosive gas concentrations. *Procedia Engineering* **47**, (2012) 224.
10. V. E. Bochenkov, G. Sergeev, Sensitivity, Selectivity, and Stability of Gas-sensitive Metal-Oxide Nanostructures. *Metal Oxide Nanostructures and Their Applications* **3**, (2010) 31.
11. A. Afonja *et al.*, Zeolites as transformation elements in discriminating semiconductor metal oxide sensors. *Procedia Engineering* **5**, (2010) 103.
12. V. Krivertsky, A. Ponzoni, E. Comini, M. Rumyantseva, A. Gaskov, Selective modified SnO2-based materials for gas sensors arrays. *Procedia Chemistry* **1**, (2009) 204.
13. P. Varsani, A. Afonja, D. E. Williams, I. P. Parkin, R. Binions, Zeolite-modified WO3 gas sensors - Enhanced detection of NO_2. *Sensors and Actuators B: Chemical* **160**, (2011) 475.
14. A. Hackner, S. Beer, G. Müller, T. Fischer, S. Mathur, Surface ionization detection of amphetamine-type illicit drugs. *Sensors and Actuators B* **162**, (2012) 209.
15. A. Hackner *et al.*, Surface ionization detection of amine containing drugs. *Sensors and Actuators B: Chemical*, (2012) 6.
16. U. D. o. Justice, Guide for the selection of drug detectors for law enforcement applications. *National Institute of Justice*, (2000) 54.
17. Z. Xu, J. Wang, Y. Long, Zeolite-based materials for gas sensors. *Sensors* **6**, (2006) 1751.
18. K. D. Schierbaum, U. Weimar, W. Göpel, R. Kowalkowski, Conductance, work function and catalytic activity of SnO_2-based sensors. *Sensors and Actuators B* **3**, (1991) 205.
19. S. M. Kanan, O. M. El-Kadri, I. A. Abu-Yousef, M. C. Kanan, Semiconducting metal oxide based sensors for selective gas pollutant detection. *Sensors* **9**, (2009) 8158.
20. K. Sahner, G. Hagen, D. Schönauer, S. Reib, R. Moos, Zeolites - versatile materials for gas sensors. *Solid State Ionics* **179**, (2008) 2416.
21. M. Vilaseca *et al.*, Gas detection with SnO_2 sensors modified by zeolite films. *Sensors and Actuators B* **124**, (2007) 99.
22. K. Arshak, E. Moore, G. M. Lyons, J. Harris, S. Clifford, A review of gas sensors employed in electronic nose applications. *Sensor Review* **24**, (2004) 181.
23. D. M. Wilson, S. Hoyt, J. Janata, K. Booksh, L. Obando, Chemical sensors for portable, handheld field instruments. *IEEE Sensors Journal* **1**, (2001) 256.
24. M. C. C. Oliveros *et al.*, Electronic nose based on metal oxide semiconductor sensors as a fast alternative for the detection of adulteration of virgin olive oilds. *Analytica Chimica Acta* **459**, (2002) 219.
25. M. Pardo, G. Sberveglieri, Classification of electronic nose data with support vector machines. *Sensors and Actuators B* **107**, (2005) 730.
26. J. L. Burgess, D. Chandler, in *Occupational, Industrial, and Environmental Toxicology*. (Mosby, Inc., Philadelphia, PA, 2003), pp. 746-765.
27. G. Man, B. Stoeber, K. Walus, An assessment of sensing technologies for the detection of clandestine methamphetamine drug laboratories. *Forensic Science International* **189**, (2009) 1.
28. J. I. Khan, T. J. Kennedy, D. R. C. Jr, *Part II Chapter 5 Forensic Language in Basic Principles of Forensic Chemistry*. (Humana Press, New York, 2012).
29. L. Wang, *Support Vector Machines: Theory and Applications*. L. Wang, Ed., (Springer, Netherlands, 2005).
30. L. Hamel, *Knowledge Discovery with Support Vector Machines*. (Wiley & sons, Canada, 2009).
31. C. Distante, N. Ancona, P. Siciliano, Support vector machines for olfactory signals recognition. *Sensors and Actuators B* **88**, (2003) 30.
32. G. F. Fine, L. M. Cavanagh, A. Afonja, R. Binions, Metal oxide semi-conductor gas sensors in environmental monitoring. *Sensors* **10**, (2010) 5469.
33. G. Korotcenkov *et al.*, Acceptor-like behavior of reducing gases on the surface of n-type In_2O_3. *Applied Surface Science* **227**, (2004) 122.
34. R. Binions *et al.*, Discrimination effects in zeolite modified metal oxide semiconductor gas sensors. *IEEE Sensors Journal* **11**, (2011) 1145.
35. Y. Zheng, Z. Li, P. K. Dutta, Exploitation of unique properties of zeolites in the development of gas sensors. *Sensors* **12**, (2012) 5170.
36. K. Wetchakun *et al.*, Semiconducting metal oxides as sensors for environmentally hazardous gases. *Sensors and Actuators B* **160**, (2011) 580.
37. H. Teterycz *et al.*, Oxidation of Hydrocarbons on the surface of tin dioxide chemical sensors. *Sensors* **11**, (2011) 4425.
38. P. Ivanov *et al.*, A route toward more selective and less humidity sensitive screen-printed SnO_2 and WO_3 gas sensitive layers. *Sensors and Actuators B* **100**, (2004) 221.
39. L. Liu *et al.*, High toluene sensing properties of NiO-SnO_2 composite nanofiber sensor operating at 330 C. *Sensors and Actuators B* **160**, (2011) 448.
40. V. Srivastava, K. Jain, Highly sensitive NH_3 sensor using Pt catalyzed silica coating over WO_3 thick films. *Sensors and Actuators B* **133**, (2008) 46.
41. X. Ma, H. Song, C. Guan, Enhanced ethanol sensing properties of ZnO-doped porous SnO_2 hollow nanospheres. *Sensors and Actuators B* **188**, (2013) 193.
42. M. Ahsan *et al.*, Low temperature response of nanostructured tungsten oxide thin films toward hidrogen and ethanol. *Sensors and Actuators B* **173**, (2012) 789.
43. K. Arshak, I. Gaidan, NiO/Fe_2O_3 polymer thick films as room temperature gas sensors. *Thin Solid Films* **495**, (2006) 286.
44. H. Kim *et al.*, Ultraselective and sensitive detection of xylene and toluene for monitoring indoor air pollution using Cr-doped NiO hierarchical nanostructures. *Nanoscale* **5**, (2013) 7066.

45. S. Santra, P. K. Guha, S. K. Ray, F. Udrea, J. W. Gardner, paper presented at the 2013 IEEE 5th International Nanoelectronics Conference (INEC), Singapore, 2013.
46. N. Kim *et al.*, Highly sensitive and selective hydrogen sulfide and toluene sensors using Pd functionalized WO_3 nanofibers for potential diagnosis of halitosis and lung cancer. *Sensors and Actuators B*, (2013) 1.

